

Importance Sampling Approach for Dynamic Stochastic Optimal Power Flow Control

Aleksander Lukashevich, Aleksander Bulkin, Roland Grinis, Ilya Makarov, and Yury Maximov

Abstract— Renewable energy sources (RES) has become common in modern power systems, helping to address decarbonization and energy security goals. Despite being attractive, RES such as solar and have low inertia and high uncertainty, thus compromising power grid stability and increasing the risk of energy blackouts. Stochastic (chance-constrained) optimization and other state-of-the-art algorithms to optimize and control power generation under uncertainty either explicitly assume the distribution of renewables, or use data-driven approximations. The latter becomes time-consuming and inaccurate, esp. when optimizing over multiple time steps.

This paper considers a discrete-time chance-constraint direct current optimal power flow control problem for minimizing power generation costs subjected to power balance and security constraints. We propose an importance-sampling-based data-driven approximation for the optimal automated generation control, which allows to improve accuracy and reduce data requirements compared to state-of-the-art methods. We support the proposed approach theoretically and empirically. The results demonstrate the approach superior performance in handling generation uncertainty, enhancing the stability of renewable-integrated power systems, and facilitating the transition to clean energy.

Index Terms— power system control, importance sampling, uncertainty, optimal power flow

I. INTRODUCTION

INTEGRATING renewable energy sources (RES) aligns with the United Nations sustainable development goals, promoting affordable and clean energy while enhancing energy security and resilience. But the integration of RES introduces significant uncertainty in power systems generation, posing challenges to existing grid optimization and control policies.

The Optimal Power Flow (OPF) [1] is a fundamental power optimization problem that aims to achieve economically optimal generation while adhering to grid security and power balance constraints. To account for generation uncertainty, the (joint) chance-constrained extension considers an unknown (joint) distribution of renewable energy sources [2], [3]. Alternatively, a robust approach, assuming bounded uncertainty, offers a more conservative solution in practice [4]–[6].

The discrete-time dynamic chance-constrained optimal power flow problem [7]–[9] models optimal generation set-points for sequential timestamps, temporarily binding generator states through ramp-up and ramp-down constraints. For fast and efficient power dispatch in bulk power systems, the automatic generation control (AGC) is commonly employed [10].

While the chance-constrained extension enhances flexibility in modeling uncertainty, solving it for an arbitrary distribution becomes computationally infeasible [11], [12]. To overcome this, data-driven approximations such as Scenario

Approximation (SA) [13] and Sample Average Approximation (SAA) [14], [15] have proven successful.

Chance-constrained formulations offer a more flexible approach to model uncertainty, allowing control over the confidence level of solution feasibility. These formulations can be represented as Joint Chance Constraints (JCC) or Single Chance Constrained (SCC) forms. While analytical solutions exist for the SCC type, they are often conservative due to the sub-additivity of the probability measure. In contrast, JCC does not allow for an analytical formulation, necessitating the use of approximations like Scenario Approximation (SA) [13] or Stochastic Average Approximation (SAA) [14], [15].

Unfortunately, these approaches become computationally prohibitive when higher accuracy approximations are required. This compromises power system operation security practices and hinders the clean energy transition. To address this challenge, this paper proposes an importance-sampling-based scenario approximation for the discrete-time optimal power flow problem. The approach significantly reduces the sample requirements compared to baseline methods, while improving accuracy. The contribution of this paper is two-fold:

- propose an importance-sampling-based scenario approximation for the discrete-time optimal power flow problem, requiring nearly half the samples of the baseline method.
- demonstrate the state-of-the-art empirical performance of our approach across various IEEE test cases.

The rest of this paper is organized as follows. Section II provides background, notation, and problem setup. Section III presents the mathematical background of the problem. In Section IV, we conduct an empirical study, and finally, Section V concludes the paper.

II. BACKGROUND AND PROBLEM SETUP

The higher-voltage direct current (DC) model is a widely used load flow model in power systems. Its simplicity for analysis arises from the linear relationships between power injections and phase angles. To describe the model, we consider a power grid given by a graph $G = (V, E)$, where V is the set of n nodes (buses) and E is the set of m lines (edges).

Let $p_g \in \mathbb{R}^{n_g}$, $p_d \in \mathbb{R}^{n_d}$, and $\theta \in \mathbb{R}^n$ be vectors representing power generations, power demands, and phase angles, respectively. Additionally, we define the vector of power injections as $p_{inj} \in \mathbb{R}^n$, where p_{inj}^i denotes the power injection at bus i , calculated as the difference between the power generation p_g^i and the power demand p_d^i at that bus. If there is no generation or demand at a bus i , either p_g^i or p_d^i is zero, respectively. The power system is balanced, so the sum of all power injections is zero, $\sum_{i \in V} p_{inj}^i = 0$.

To maintain clarity, we designate one bus as the slack bus, with its phase angle set as $\theta_s = 0$. The power injection

TABLE I: Paper notation.

\mathcal{F}	Feas. set of CC Prob. 4	n_g	number of generators
P	reliability set, $p: Wp \leq b$	n_d	number of demand nodes
E	set of lines, $ E = m$	D_i	$p \sim \mathcal{N}(\mu, \Sigma)$ s.t. $p^\top \omega^i > b_i$
V	set of buses, $ V = n$	π	feasibility prob., $p \in P$
B	$n \times n$ admittance matrix	χ	DC-OPF variables, (θ, p_g)
p_g^i, p^i	power gen. at bus i		in the mixture, $x \in X \subseteq \mathbb{R}^J$
$\underline{p}_g^i, \bar{p}_g^i$	lower/upper gen. limit	N	number of samples
\bar{D}	mixture distribution	$\mathbb{P}, \mathbb{E}, \mathbb{V}$	prob., expectation, variance
R	ramp-up/down limits	$\mathcal{N}(\mu, \Sigma)$	Gauss. distribution with
ξ^t	total uncertainty at time t	f_D	mean μ , covariance Σ
θ_i	phase angle at bus i	Φ	density of the mixture
θ_{ij}	phase angle difference	$U(0, 1)$	$\mathcal{N}(0, 1)$ distribution CDF
θ_{ij}	angle difference limits	B	uniform (0, 1) distribution
I_n	$n \times n$ identity matrix	$c(p)$	imaginary of admitt. mat.
J	number of constraints	w_i	convex cost function
D_i	Gaussian dist. conditioned on plane i	α	weight of D_i
			gen. participation factors

vector p_{inj} is related to the phase angle vector θ through an admittance matrix $B \in \mathbb{R}^{n \times n}$ as $p_{inj} = B\theta$. The components of B , denoted as B_{ij} , are non-zero if there is a line between buses i and j . For each node i , B_{ii} is defined as the negative sum of the off-diagonal elements B_{ij} with $j \neq i$, resulting in a Laplacian matrix structure.

The DC power flow equations and the associated constraints are expressed as follows:

$$p_{inj} = B\theta \quad (1a)$$

$$\underline{p}_g^i \leq p_g^i \leq \bar{p}_g^i, i \in V \text{ and } |\theta^i - \theta^j| \leq \bar{\theta}^{ij}, (i, j) \in E. \quad (1b)$$

$$\sum_{i=1}^{n_g} p_g^i = \sum_{i=1}^{n_d} p_d^i \quad (1c)$$

These equations represent the DC power flow and enforce generation and reliability constraints. The reliability constraints (1b) define a polytope P in the space of power generations, where P is given by $P = p_g : Wp_g \leq b$. Violations of reliability constraints occur when power injections p_g do not belong to this polytope P . The matrices $W \in \mathbb{R}^{J \times n_g}$ and vector $b \in \mathbb{R}^J$ can be derived from the set of DC power flow equations. We leave out relevant bulky equations to meet the paper length requirements.

The objective is to solve the power flow problem by minimizing a convex cost function $c(p)$ subject to the constraints specified in Eqs. (1a) and (1b). The function $c(p)$ captures the cost associated with the power flow generation in the system.

Table I summarizes the paper notation. We use upper indices for elements of vectors and matrices, lower-case letters for probability density functions (PDFs), and upper-case letters for cumulative distribution functions (CDFs). Once it does not lead to confusion, we use $\mathbb{P}, \mathbb{E}, \mathbb{V}$ for probability, expectation, and variance without explicitly mentioning a distribution.

III. OPTIMAL CONTROL UNDER UNCERTAINTY

In this section, we formulate the multistage chance-constrained DC-OPF. We begin by describing the fluctuations that introduce uncertainty into the system, their origins, and their significance in control and optimization. Next, we address the concept of Automated Generation Control (AGC). Further,

we present the chance-constrained optimization problem. Accordingly, we introduce and analyze the Scenario Approximation (SA) for the chance constrained control. Finally, we address and define the redundant scenarios for this problem and present a procedure to efficiently sample them.

A. Fluctuations and AGC

Power systems fluctuations typically occur both on the generation and demand side and arise from the intermittency of renewable energy generation, unstable demand from the customers, and intra-day electricity trading. Often the distribution of such fluctuations can be recovered based on historical data [16], [17]. Below we assume that the fluctuations are Gaussian with the mean and covariance recoverable from historical data [16], [18].

Next, we address the fluctuations impact the feasibility set of the DC-OPF, see Eq. (1). These fluctuations are involved the power balance equation (1c) and typically managed through primary and secondary control [19]. In this paper, we consider linear Automatic Generation Control (AGC). In our model, the generation and demand fluctuate as $(p_g^i)^t + (\xi_g^i)^t$ at bus $i = 1, \dots, n_g$ and $p_d^j + (\xi_d^j)^t$ at node $j = 1, \dots, n_d$ resp. As we assume that the initial generation is balanced, i.e., $\sum_{i=1}^{n_g} (p_g^i)^0 = \sum_{i=1}^{n_d} p_d^i$, the purpose of AGC is to balance the aggregated uncertainty term $\xi^t = \sum_{i=1}^{n_g} (\xi_g^i)^t - \sum_{i=1}^{n_d} (\xi_d^i)^t$, where ξ^t is distributed as the sum of all the nodes' uncertainties. For example, if the uncertainties are independent and identically distributed (i.i.d) Gaussians with mean $\mu = 0$ and some variance σ^2 , then ξ^t follows a Gaussian distribution $\mathcal{N}(0, (n_g + n_d) \cdot \sigma^2)$. Following [16], [20], [21], the AGC recourse brings the generation to a new setpoint $p_g^{t+1} = p_g^t + \alpha \xi^t$. In the latter the participation factors $\alpha \in \mathbb{R}^{n_g}$ satisfy $\alpha \geq 0$, $\mathbf{1}^\top \alpha = 1$. It is easy to check that if the system is initially balanced, then the new generation set-point also ensures a balanced system. The power mismatch at timestamp $t = 1, \dots, T$ is given by:

$$\mathbf{1}^\top p^t - \mathbf{1}^\top p_d - \xi^t = \mathbf{1}^\top p^{t-1} - \mathbf{1}^\top p_d + \xi^t - \xi^t = 0. \quad (2)$$

i.e., this control strategy keeps the system balanced. Notice that ξ^t represents the overall fluctuation, including load and generation uncertainties, and p_d remains constant in time.

B. Chance constrained multi-stage control

We consider an uncertain discrete-time dynamical system with T , $T < \infty$, timestamps, and ξ^t , $1 \leq t \leq T$, total power mismatch due to uncertainties. Below, we use p instead of p_g to simplify the notation. We assume that ξ^t are distributed normally and represent the total power mismatch in the system at timestamp t . Below we consider the linear Automatic Generation Control (AGC) [22]: $p^t = p^{t-1} + \alpha \xi^t$, where $\alpha \in \mathbb{R}^{n_g}$ is a vector of the participation factors $\alpha_k \geq 0$, $\sum_{1 \leq k \leq n} \alpha_k = 1$, and ξ^t is a one dimensional random variable representing total disbalance at time step t . We assume that for balancing the system generator i contributes proportionally to its participation factor α_i for each t , $1 \leq t \leq T$. We would use vector and scalar notation interchangeably later in the paper if it does not lead to confusion. We assume the power system is balanced at the initial time step $t = 0$, i.e., $\mathbf{1}^\top p^0 = \mathbf{1}^\top p_d$.

Thus, with the linear AGC the system remains balanced at each timestamp, as it was shown at the end of Section III-A.

We assume uncertainties being uncorrelated in time and follow the Gaussian distribution, $\xi^t \sim \mathcal{N}(0, (\sigma^t)^2)$, $1 \leq t \leq T$. In practice, the ramp rates of generators are limited as

$$|p_i^t - p_i^{t-1}| \leq R_i, \quad R_i > 0. \quad (3)$$

The discrete-time dynamic chance-constrained optimization problem is as follows:

$$\begin{aligned} & \min_{p^t, \alpha} \mathbb{E} \sum_{t=1}^T c(p^t) \\ & \text{subject to:} \\ & \mathbb{P} \left(\begin{array}{l} Wp^t \leq b, 1 \leq t \leq T \\ p^t = p^{t-1} + \alpha \xi^t, 1 \leq t \leq T \\ |p_k^t - p_k^{t-1}| \leq R_k, 1 \leq k \leq n_g \end{array} \right) \geq 1 - \eta. \end{aligned} \quad (4)$$

where $0 < \eta < 1$, \mathbb{P} is a joint measure induced by the uncertainty distribution, and α is a set of participating factors.

An equivalent formulation to the problem above is

$$\begin{aligned} & \min_{p^t, \alpha} \mathbb{E} \sum_{t=1}^T c(p^t) \\ & \text{subject to:} \\ & \mathbb{P} \left(\begin{array}{l} Wp_0 + W\alpha \sum_{t \leq \tau} (\xi^t) \leq b, 0 \leq \tau \leq T \\ |\alpha_k \xi^t| \leq R_k, 1 \leq k \leq n_g \end{array} \right) \geq 1 - \eta. \end{aligned} \quad (5)$$

where for $t = 0$ we assume no uncertainty, i.e., $\xi^0 = 0$.

C. Scenario approximation of chance constrained control

A (convex) Scenario Approximation to the problem above is

$$\begin{aligned} & \min_{p^0, \alpha} c(p^0) \\ & \text{subject to:} \\ & Wp_0 + W\alpha \sum_{t \leq \tau} \xi^t(j) \leq b, 0 \leq \tau \leq T \\ & |\alpha_k \xi^t(j)| \leq R_k, 1 \leq k \leq n_g \end{aligned} \quad (6)$$

with scenarios $\xi^t(j) \sim \mathcal{N}(0, (\sigma^t)^2)$, $1 \leq j \leq N$. We omit expectation in the cost function since for typical cost functions in power systems (quadratic and linear, with diagonal matrix in quadratic term) the cost remains the same (in terms of p^0) after taking expectation, provided the uncertainty has zero mean.

Scenario approximation (SA) is very attractive from the practical perspective but requires an extreme number of samples to get reasonable accuracy [13]. Importance sampling helps to reduce the SA computational burden [23]–[25] in chance-constrained optimization; however, it has not yet been studied for dynamic power flow optimization problems.

The importance sampling approach we leverage in this paper consists of two steps. First, we derive a conservative outer approximation to the set of optimal solutions of Problem (5). Based on this, we add a sequence of deterministic constraints to eliminate redundant scenarios from the scenario approximation. Finally, instead of using vanilla Monte-Carlo, we sample from a proxy (importance) distribution having less redundant scenarios. This approach improves the sample complexity and reliability [23].

The paper extends the importance sampling based scenario approximation to discrete-time dynamic chance-constrained optimization and verifies the empirical performance of this approach over the optimal power flow problem.

D. Redundant scenarios

We now formulate the polytope that contains the samples that are not able to drive the system out of the safe operating zone during T snapshots. We will use the notion of a *redundant* scenario.

Definition 1: Let $\vec{\xi}^t(j)$, $j = 1, \dots, N$, be scenarios drawn from $\mathcal{N}(0, \text{diag}((\sigma^1)^2, \dots, (\sigma^T)^2))$. A scenario $\vec{\xi}(j)$ is called redundant if the solution of a scenario approximation remains the same even when it is excluded from the latter.

Further, we develop an approximation of the set of redundant scenarios for the current optimal control problem.

The participation factors α for secondary control are often fixed, enabling long-term grid stability and fast corrective secondary control [19]. However, in practice, small deviations from the long-term optimal point α^0 , where $|\alpha - \alpha^0|_2 \leq \delta\alpha$, are economically advantageous. Based on that assumption, we derive the proxy distribution for efficient scenario generation.

Lemma 1: Let AGC control be $p^t = p^{t-1} + \alpha \xi^t$. Then $p^t - p^{t-1}$ is either in the positive or negative orthant.

Proof: Recall that $\{\alpha : \sum_{k=1}^{n_g} \alpha_k^\top \mathbf{1} = 1, \alpha \geq 0\}$. Thus, since ξ^t is a scalar, $\alpha \xi^t$ has either all positive or all negative components. \blacksquare

The generation adjustments $\alpha \xi^t$ can only either decrease or increase all current powers p^{t-1} as illustrated in Fig. 1c. Moreover, since the variance of $\sum_{\tau \leq t} \xi^\tau$ grows in time as shown in Fig. 2, the probability of failure for each operating point is increasing.

Our next step is to derive an upper bound for the failure probability of a control strategy (ξ^1, \dots, ξ^T) , α with a given starting point p^0 . To achieve this, we utilize the following bounds on the probability of $\mathbb{P}(S_1 \cup \dots \cup S_k)$ for some arbitrary sets $S_1, \dots, S_k : \max_{i \leq k} \mathbb{P}(S_i) \leq \mathbb{P}(S_1 \cup \dots \cup S_k) \leq \sum_{i \leq k} \mathbb{P}(S_i)$.

Let us consider the probability that all system states are feasible with a prescribed probability at least $1 - \eta$:

$$\pi = \mathbb{P} (\forall k, t : \omega_k^\top p^t \leq \beta_k, k \leq n, t \leq T),$$

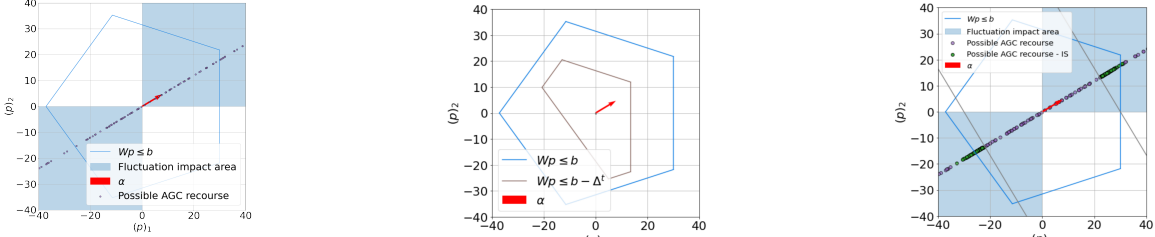
note that $\pi \leq 1 - \max_{k \leq n, t \leq T} \mathbb{P}(\omega_k^\top p^t > \beta_k)$ and $\mathbb{P}(\forall i, t : \bigcup_i \omega_i^\top p^t > \beta_i) \leq 1 - \max_{i, t} \mathbb{P}(\omega_i^\top p^t > \beta_i)$ with $p^t \sim \mathcal{N}(p^0, \text{diag}((\sigma^1)^2, \dots, \sum_{t=1}^{T-1} (\sigma^t)^2))$. Now, we have the upper bound π greater or equal than $1 - \eta$ we get

$$\max_{i, t} \mathbb{P}(\omega_i^\top p^t > \beta_i) \leq \eta. \quad (7)$$

We use this necessary feasibility condition to get the outer approximation of the Joint Chance Constraint (JCC) in Eq. (5).

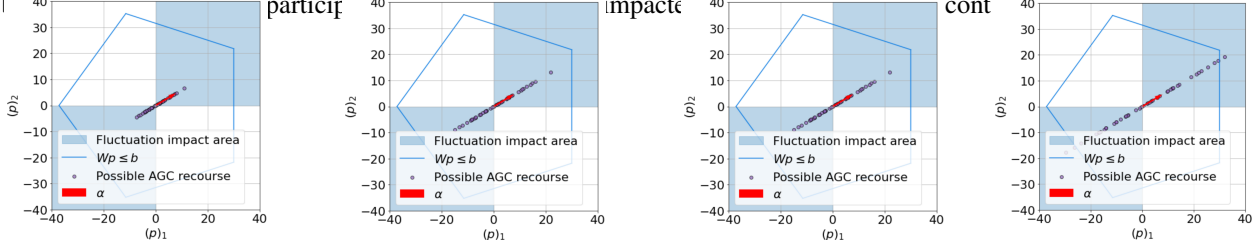
We will now derive the *outer* approximation of the JCC feasibility set based on the necessary condition. It is important to note that if there exists a timestamp t in the range of 1 to T and a plane ω_i in the range of 1 to J , such that the necessary feasibility condition (7) does not hold, it implies that the entire JCC, Prob. (5), cannot be satisfied.

Thus, assuming that for some t, i (7) is violated and recalling that $p^t = p^0 + \alpha \zeta^t$, $\zeta^t = \sum_{\tau=1, \dots, t-1} \xi^\tau$, $\zeta^t \sim$



(a) The interior of the blue polytope is feasible; possible gener. setpoints are in brown. (b) The deterministic feasibility polygon. (c) Controls resulted from AGC dispatch after eliminating redundant scenarios.

Fig. 1: The results of AGC dispatch and feasibility sets. Notice, that Δ_i^t depends on $|\omega_i^\top \alpha|$. Indeed, the planes that are closer to 1



$\mathcal{N}(0, (\tilde{\sigma}^t)^2)$, with $(\tilde{\sigma}^t)^2 = \sum_{\tau=1}^{t-1} (\sigma^\tau)^2$, we get for a plane with $\omega_i^\top \alpha \neq 0$: $\mathbb{P}(\omega_i^\top p^0 + \omega_i^\top \alpha \zeta^t > \beta_i) > \eta \implies \Phi\left(\frac{\omega_i^\top p^0 - \beta_i}{\tilde{\sigma}^t \|\omega_i^\top \alpha\|}\right) > \eta$. The latter expression defines a complement of the polytope $\mathcal{P}_{out} = \{p : \omega_i^\top p \leq \beta_i - \Delta_i^t \|\omega_i^\top \alpha\|\}$, where $\Delta_i^t = \Phi^{-1}(1 - \eta)\tilde{\sigma}^t$. Essentially, \mathcal{P}_{out} defines a necessary feasibility polytope for the original chance-constrained feasibility set. Note that those hyperplanes that are orthogonal to the AGC participation factors vector α , $\omega_i^\top \alpha = 0$, cannot be violated as a result of the AGC action. Moreover, right-hand sides of the inequalities decrease from deterministic β_i as $\tilde{\sigma}^t = \sqrt{\sum_{\tau=1}^{t-1} (\sigma^\tau)^2}$ grows. Figure 1c illustrates the mutual geometry between initial feasibility polytope and necessary feasibility polytope at $t > 1$.

Remark 1: Additionally, the same reasoning applies to the ramp-up and ramp-down constraints $|\alpha_k \xi^t| \leq R_k$. In this case, the logic remains unchanged for the hyperplanes $\alpha_i \xi^t \leq R_i$. It's important to note that $|\alpha_k \xi^t| \leq R_k$ is equivalent to the simultaneous satisfaction of $\alpha_k \xi^t \leq R_k$ and $-\alpha_k \xi^t \leq R_k$.

To derive efficient samples for scenario approximation considering AGC recourse and constraint satisfaction, we need to impose conditions on sample redundancy. At timestamp t , we have the condition $\omega_i^\top p^0 + \omega_i^\top \alpha \zeta^t \leq \beta_i$. If a scenario $\zeta^t(j)$ satisfies $\omega_i^\top \alpha \zeta^t(j) \leq \Phi^{-1}(1 - \eta) \|\omega_i^\top \alpha\| \tilde{\sigma}^t$, it implies that the initial generation should satisfy $\omega_i^\top p^0 \leq \beta_i - \omega_i^\top \alpha \zeta^t(j)$. However, this right-hand side is looser than $\beta_i - \Phi^{-1}(1 - \eta) \|\omega_i^\top \alpha\| \tilde{\sigma}^t$, meaning that even the necessary feasibility condition would not be satisfied. Thus, the scenario $\zeta^t(j)$ with $\omega_i^\top \alpha \zeta^t(j) \leq \Phi^{-1}(1 - \eta) \|\omega_i^\top \alpha\| \tilde{\sigma}^t$ is redundant.

To get efficient samples for scenario approximation, one must sample $\zeta^t(j)$ outside of the polytope $\mathcal{P}_r = \{(\zeta^1, \dots, \zeta^T)^\top : \omega_i^\top \alpha \zeta > \Phi^{-1}(1 - \eta) \|\omega_i^\top \alpha\| \tilde{\sigma}^t, \forall t, \forall i\}$.

The polytope can equally be described as $\mathcal{P}_r =$

$\{\zeta : \mathcal{W}\zeta \leq \Phi^{-1}(1 - \eta)\mathcal{S}\}$. Here $\mathcal{W} \in \mathbb{R}^{(J \cdot T) + (2 \cdot n_g \cdot T) \times T}$ is a block diagonal matrix. The j^{th} block of the matrix is of a shape $T \times T$ and $\mathcal{W}_j = \text{sign}(\omega_k^\top \alpha) \cdot I$ where $j \in 1 + (k - 1) \cdot T, \dots, k \cdot T$, $k = 1, \dots, J$. The other blocks correspond to the ramp-up/down constraints. They are as follows: $\mathcal{W}_j = I$ for $j \in J \cdot T + 1 + (k - 1) \cdot T, \dots, J \cdot T + 1 + k \cdot T$ and $k = 1, \dots, n_g$. The remaining blocks of the matrix are the same except the sign and correspond to the ramp-down constraints. The vector on right-hand side is $\mathcal{S} = (\mathcal{S}_W, \mathcal{S}_{ramp})$, where $\mathcal{S}_W = (\tilde{\sigma}^1, \dots, \tilde{\sigma}^T, \dots, \tilde{\sigma}^1, \dots, \tilde{\sigma}^T)$ and $\mathcal{S}_{ramp} = \left[\frac{R_1}{\alpha_1 \sigma^1}, \dots, \frac{R_{n_g}}{\alpha_{n_g} \sigma^1}, \dots, \frac{R_1}{\alpha_1 \sigma^T}, \dots, \frac{R_{n_g}}{\alpha_{n_g} \sigma^T} \right]$, $\mathcal{S} \in \mathbb{R}^{J \cdot T + 2 \cdot n_g \cdot T}$.

E. Sampling non-redundant scenarios

In order to sample non-redundant scenarios, we approximate their distribution with a mixture of distributions D that has the density $f_D(x) = \sum_{i=1}^{|S|} w_i f_{D_i}(x)$. Here $|S| = J \cdot T + 2 \cdot n_g \cdot T$, mixture components' weights are positive and $\sum_i w_i = 1$, f_{D_i} are mixture components densities. The mixture components are Gaussians conditioned outside of the plane i : $x \sim D_i \iff \mathcal{N}(0, \Sigma_\zeta)$, $\mathcal{W}_i^\top x > \mathcal{S}_i$, where $\Sigma_\zeta = \text{diag}((\tilde{\sigma}^1)^2, \dots, (\tilde{\sigma}^T)^2)$. The exact expression for the density is $f_{D_i} = \mathbf{1}(\mathcal{W}_i^\top x > \mathcal{S}_i) f(x) / \mathbb{P}(\mathcal{W}_i^\top x > \mathcal{S}_i)$, where the probability also has explicit expression: $\mathbb{P}(\mathcal{W}_i^\top x > \mathcal{S}_i) = \Phi(-\mathcal{S}_i / \|\Sigma_\zeta^{1/2} \mathcal{W}_i\|)$. Such mixture has proven to be useful in approximating the distribution of interest [23], [24], [17]. For this study, we use $w_1 = \dots = w_{|S|}$. To sample from this mixture, one must pick a plane with probability w_i and then sample outside of this plane. The Algorithm 1 summarizes the procedure to produce samples outside of a plane of \mathcal{P}_r .

With the obtained samples $\zeta^t(j)$ where $j = 1, \dots, N$ and $t = 1, \dots, T$, we construct the scenario approximation 6. Fig. 1c illustrates the difference between the samples obtained from

the importance sampling procedure described above and the classical Monte Carlo (MC) sampling.

Algorithm 1 Sampling $p \sim \mathcal{N}(\mu, \Sigma)$ s.t. $p^\top \omega_i \geq b_i$

Input: Mean μ , covariance Σ , and a constraint $p^\top \omega^i \leq b_i$.

Output: $p \sim \mathcal{N}(\mu, \Sigma)$ s.t. $p^\top \omega^i \geq b_i$

- 1: Sample $z \sim \mathcal{N}(0, I_n)$ and $u \sim U(0, 1)$
- 2: Compute $y = \Phi^{-1}(\Phi(\tau) + u(1 - \Phi(\tau)))$
- 3: Set $\phi = \bar{\phi}y + (I_n - \bar{\phi}\bar{\phi}^\top)z$, with $\bar{\phi} = \Sigma^{1/2}\omega^i / \|\Sigma^{1/2}\omega^i\|_2$
- return** $p = \Sigma^{1/2}(\phi + \mu)$

IV. EMPIRICAL STUDY

A. Algorithms and Implementation Details

We compare the performance of scenario approximations based on different sampling strategies: classical Monte-Carlo (SA) and the proposed Importance Sampling (SA-IS). For our test cases, we consider power systems from MATPOWER [26] (Washington-14, IEEE-30, and IEEE-57). We implemented¹ the methods using Python 3.9.13 and PandaPower 2.8.0 [27] on a MacBook Pro (M1 MAX, 64 GB RAM). We use CVX [28] and HiGHs [29] optimization solvers.

B. Test Cases and Numerical Results

We studied the solutions of the scenario-based chance-constrained optimal power flow problem, considering Gaussian fluctuations, for both the classical Monte-Carlo strategy (SA) and the proposed Importance Sampling-based scenario generation (SA-IS). The comparisons were made for three different test cases: Washington-14, IEEE-30, and IEEE-57 bus systems, which have 14, 30, and 57 buses/nodes, respectively. In all cases, we assumed that the power generation and consumption levels fluctuated with a standard deviation of 0.01 of their nominal values. Thus, $\zeta^t \sim \mathcal{N}(0, (\tilde{\sigma}_t^2)^2)$, where $\tilde{\sigma}_t^2 = 0.01 \cdot t \cdot n_g$. We simulated for $T = 5$ snapshots.

The main point of comparison between SA-IS and classical SA is the number of samples N required to obtain a solution with a reliability of δ . The value of $1 - \eta$ stands for the required confidence threshold for linear constraints, $1 - \delta$ for the reliability of the SA solution; see Sec. III for details.

To evaluate the empirical estimation of the solution reliability $\hat{\delta}$, we independently construct $L = 200$ different scenario approximations for both SA and SA-IS with N samples. For each approximation, we obtain L different solutions: $(x_N^*)_l$, $l = 1, \dots, L$. Next, we estimate the confidence of each obtained solution over 10^4 Monte-Carlo samples to get $(\hat{P}_N)_l$, $l = 1, \dots, L$. Finally, the reliability of a solution is estimated by $1 - \hat{\delta}$, which represents the fraction of L solutions $(x_N^*)_l$ such that $(\hat{P}_N)_l \geq 1 - \eta$. See Alg. 2 for details.

We provide the number of samples required to reach confidence thresholds of $1 - \eta = 0.95$ and 0.99 with reliability of 0.99 for SA-IS and SA in Table II: the number of samples required is 30-50% less for SA-IS compared to classical SA. Furthermore, the advantage of SA-IS becomes more substantial as the increase of $1 - \eta$.

To better illustrate the dependency between number of samples in the approximation N and reliability estimates $1 - \hat{\delta}$,

Algorithm 2 $\hat{\delta}$ – an empirical estimate

Require: L – number of trials, DC-OPF problem parameters, η – confidence level, N_0 – initial size of scenario approximation, N_{\max} – maximal size of scenario approximation

$$N \leftarrow N_0$$

$$\hat{\delta} \leftarrow \text{storage for } \hat{\delta}_N$$

while $N \leq N_{\max}$ **do**

$$C_N \leftarrow 0 \text{ – feasibility counter}$$

$$l \leftarrow 1$$

while $l \leq L$ **do**

$$\text{Get } (x_N^*)_l \text{ with SA-IS or SA using Eq. (6)}$$

$$\text{Get constraint satis. prob. } (\hat{P}_N)_l \text{ using Monte Carlo}$$

$$\text{if } (\hat{P}_N)_l \geq 1 - \eta \text{ then } C_N \leftarrow C_N + 1$$

$$\text{end if}$$

end while

$$1 - \hat{\delta}_N \leftarrow C_N / L \text{ – fraction of trials is feasible}$$

$$\text{Append } \hat{\delta}_N \text{ to } \hat{\delta}$$

$$n \leftarrow n + N_{\max} / 10$$

end while

return $\hat{\delta}$

Case	η	SA No	SA Cost	IS-SA No	IS-SA Cost	DC-OPF Cost
grid14	0.05	93	5.5e+03 ± 1.2e-11	93	5.5e+03 ± 5.5e-12	5.2e+03
grid30	0.05	93	6.0e+03 ± 2.8e-11	93	6.3e+03 ± 1.3e-11	5.7e+03
grid57	0.05	93	2.5e+04 ± 4.4e-11	93	2.5e+04 ± 4.4e-11	2.5e+04
grid14	0.01	363	5.6e+03 ± 1.5e-11	93	5.5e+03 ± 1.5e-11	5.2e+03
grid30	0.01	363	6.2e+03 ± 4.5e-12	183	6.1e+03 ± 4.5e-12	5.7e+03
grid57	0.01	453	2.5e+04 ± 4.4e-11	363	2.5e+04 ± 4.0e-11	2.5e+04

TABLE II: The number of samples for SA-IS and SA required in CC-OPF with a confidence threshold of $1 - \eta$ to achieve the empirical reliability of $1 - \hat{\delta} = 0.99$. The value of $1 - \eta$ is given by out-of-sample Monte Carlo; the empirical reliability is given by averaging over $L = 100$ independent CC-OPF problem instances, as described in Alg. 2.

we demonstrate Fig. 3d. We illustrate the dependence between empirical reliability $1 - \hat{\delta}$ and N over a range of values for the IEEE 118 bus system in Fig. 3d. Here, we keep a confidence threshold of joint chance constraint feasibility $1 - \eta = 0.99$. In addition to SA-IS and SA. Moreover, we present box-plots for the spread of $(\hat{P}_N)_l$ for different N , in Fig. 3a. We denote $(\hat{P}_N)_l$ as the probability of constraint satisfaction, empirically computed using 10^4 Monte Carlo samples of Algorithm 2, see Eq. 8. Note that SA-IS reaches a higher reliability level $(1 - \hat{\delta})$ with a substantially fewer number of samples N . These boxplots indicate that the variance in the obtained solution's chance-constraint feasibility reduces faster for SA-IS, noted by thinner boxplots and lack of outliers, compared to SA.

V. CONCLUSION

Importance sampling emerges as a valuable tool for real-time reliability assessment in power grids. In this study, we present an algorithm that, firstly, constructs a physics-informed mixture distribution for importance sampling, and, secondly, employs convex optimization to fine-tune the weights of this mixture. The proposed method surpasses existing state-of-the-art algorithms in terms of both accuracy and efficiency for reliability assessment. This approach can be extended and applied to various uncertain optimization and control problems further enhancing their stability and performance.

¹<https://urlr.me/crdtR>

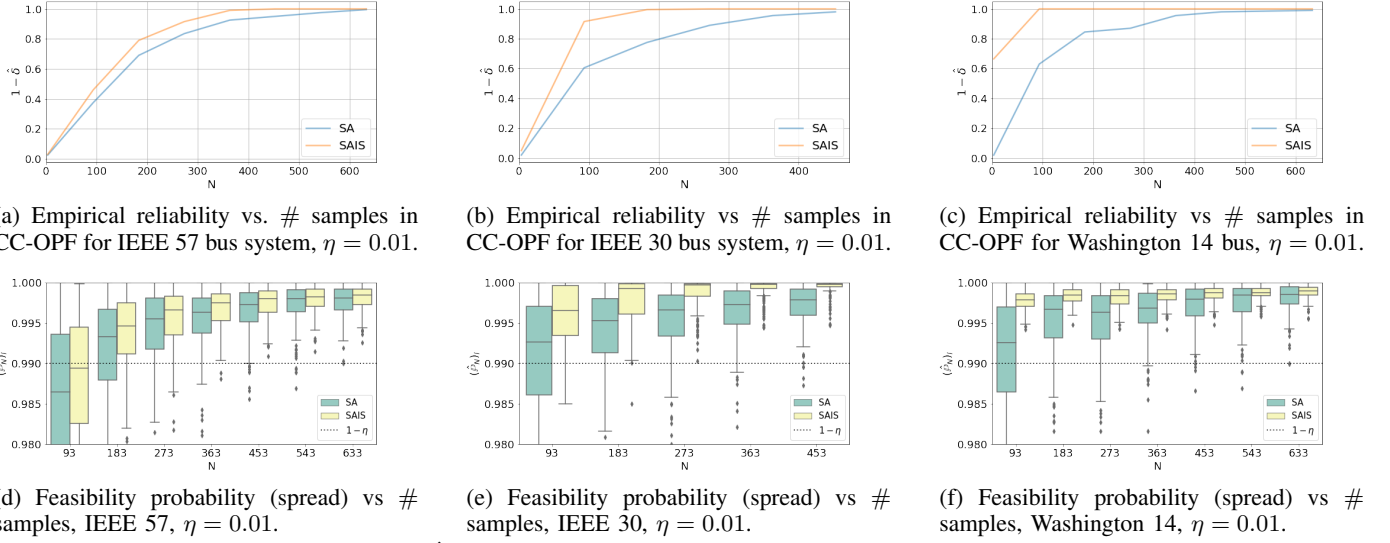


Fig. 3: (a, b, c) Empirical reliability ($1 - \hat{\delta}$) and (d, e, f) the probability of constraints feasibility ($25\% - 75\%$ interquartile range, IQR) $(\hat{P}_N)_l$ for CC-OPF ($1 - \eta = .99$) in the IEEE 57 & 30, Washington 14 systems. The empirical estimates are computed with $L = 200$ optimization instances (for $1 - \hat{\delta}$), and $N_{MC} = 10^4$ Monte-Carlo samples for each instance to determine constraint validation (for box-plot of $(\hat{P}_N)_l$), as described in Alg. 2. Notice that the SA-IS requires much less number of samples compared to SA or SA-O.

REFERENCES

[1] B. Stott and O. Alsaç, “Optimal power flow: Basic requirements for real-life problems and their solutions,” in *SEPOPE XII Symposium, Rio de Janeiro, Brazil*, vol. 11, 2012, pp. 1–10.

[2] X. Geng and L. Xie, “Data-driven decision making in power systems with probabilistic guarantees: Theory and applications of chance-constrained optimization,” *Ann. rev. in control*, vol. 47, pp. 341–363, 2019.

[3] D. Bienstock, M. Chertkov, and S. Harnett, “Chance-constrained optimal power flow: Risk-aware network control under uncertainty,” *Siam Review*, vol. 56, no. 3, pp. 461–495, 2014.

[4] A. A. Sousa, G. L. Torres, and C. A. Canizares, “Robust optimal power flow solution using trust region and interior-point methods,” *IEEE Trans. on Power Systems*, vol. 26, no. 2, pp. 487–499, 2010.

[5] A. Ben-Tal and A. Nemirovski, “Robust optimization—methodology and applications,” *Mathematical programming*, vol. 92, pp. 453–480, 2002.

[6] T. Ding, Z. Bie, L. Bai, and F. Li, “Adjustable robust optimal power flow with the price of robustness for large-scale power systems,” *IET Generation, Transmission & Distrib.*, vol. 10, no. 1, pp. 164–174, 2016.

[7] X. Lou, J. Zhang, C. Guo, H. Tao, C. Yang, and J. Zhang, “Multi-stage security constrained opf using dynamic thermal rating,” in *2019 IEEE Power & Energy Society General Meeting*. IEEE, 2019, pp. 1–5.

[8] F. Capitanescu and L. Wehenkel, “Improving the statement of the corrective security-constrained optimal power-flow problem,” *IEEE Trans. on Power Systems*, vol. 22, no. 2, pp. 887–889, 2007.

[9] A. Monticelli, M. Pereira, and S. Granville, “Security-constrained optimal power flow with post-contingency corrective rescheduling,” *IEEE Trans. on Power Systems*, vol. 2, no. 1, pp. 175–180, 1987.

[10] F. Xu, Z. Gao, Q. Ding, and M. Tu, “The real time generation scheduling model considering automatic generation control,” in *2017 IEEE E2 Conference*. IEEE, 2017, pp. 1–6.

[11] A. Nemirovski, “On safe tractable approximations of chance constraints,” *European Journal of Operational Research*, vol. 219, no. 3, pp. 707–718, 2012.

[12] M. Jia, G. Hug, and C. Shen, “Iterative decomposition of joint chance constraints in opf,” *IEEE Trans. on Power Systems*, vol. 36, no. 5, pp. 4836–4839, 2021.

[13] G. C. Calafiore and M. C. Campi, “The scenario approach to robust control design,” *IEEE Trans. on automatic control*, vol. 51, no. 5, pp. 742–753, 2006.

[14] S. Ahmed and A. Shapiro, “Solving chance-constrained stochastic programs via sampling and integer programming,” in *State-of-the-art decision-making tools in the information-intensive age*. Informs, 2008, pp. 261–269.

[15] S. Sen, “Relaxations for probabilistically constrained programs with discrete random variables,” *Operations Research Letters*, vol. 11, no. 2, pp. 81–86, 1992.

[16] L. Roald and G. Andersson, “Chance-constrained ac optimal power flow: Reformulations and efficient algorithms,” *IEEE Trans. on Power Systems*, vol. 33, no. 3, pp. 2906–2918, 2017.

[17] A. B. Owen, Y. Maximov, and M. Chertkov, “Importance sampling the union of rare events with an application to power systems analysis,” *Electronic Journal of Statistics*, vol. 13, no. 1, pp. 231–254, 2019.

[18] M. Anvari, G. Lohmann, M. Wächtler, P. Milan, E. Lorenz, D. Heinemann, M. R. R. Tabar, and J. Peinke, “Short term fluctuations of wind and solar power systems,” *New J. of Phys.*, vol. 18, no. 6, p. 063027, 2016.

[19] J. Machowski, Z. Lubosny, J. W. Bialek, and J. R. Bumby, *Power system dynamics: stability and control*. John Wiley & Sons, 2020.

[20] S. Baros, Y. C. Chen, and S. V. Dhopde, “Examining the economic optimality of automatic generation control,” *IEEE Trans. on Power Systems*, vol. 36, no. 5, pp. 4611–4620, 2021.

[21] I. Mezghani, S. Misra, and D. Deka, “Stochastic ac optimal power flow: A data-driven approach,” *Electric Power Systems Research*, vol. 189, p. 106567, 2020.

[22] F. De Mello and J. Undrill, *Automatic Generation Control*, 1983.

[23] A. Lukashevich, V. Gorchakov, P. Vorobev, D. Deka, and Y. Maximov, “Importance sampling approach to chance-constrained dc optimal power flow,” *arXiv preprint arXiv:2111.11729*, 2021.

[24] A. Lukashevich and Y. Maximov, “Power grid reliability estimation via adaptive importance sampling,” *IEEE Control Systems Letters*, vol. 6, pp. 1010–1015, 2021.

[25] M. Mitrovic, O. Kundacina, A. Lukashevich, S. Budennyy, P. Vorobev, V. Terzija, Y. Maximov, and D. Deka, “Gp cc-opf: Gaussian process based optimization tool for chance-constrained optimal power flow,” *Software Impacts*, vol. 16, p. 100489, 2023.

[26] R. D. Zimmerman, C. E. Murillo-Sánchez, and R. J. Thomas, “Matpower: Steady-state operations, planning, and analysis tools for power systems research and education,” *IEEE Trans. on power systems*, vol. 26, no. 1, pp. 12–19, 2010.

[27] L. Thurner, A. Scheidler, F. Schäfer, J. Menke, J. Dollichon, F. Meier, S. Meinecke, and M. Braun, “Pandapower — an open-source python tool for convenient modeling, analysis, and optimization of electric power systems,” *IEEE Trans. on Power Syst.*, vol. 33, no. 6, pp. 6510–6521, 2018.

[28] S. Diamond and S. Boyd, “Cvxpy: A python-embedded modeling language for convex optimization,” *The Journal of Machine Learning Research*, vol. 17, no. 1, pp. 2909–2913, 2016.

[29] Q. Huangfu and J. J. Hall, “Parallelizing the dual revised simplex method,” *Math. Prog. Computation*, vol. 10, no. 1, pp. 119–142, 2018.

APPENDIX

First, we get an explicit expression for matrix W , $P = \{Wp_g \leq b\}$. Let $\chi \in \mathbb{R}^{n_\chi}$, where $n_\chi = n + n_g$, be the vector of variables describes the power system. For DC-OPF, $\chi = (\theta, p_g)^\top$. Let $A_{eq} \in \mathbb{R}^{m_{eq} \times n_\chi}$ and $b_{eq} \in \mathbb{R}^{m_{eq}}$ be a matrix and a right-hand side vector that define equality constraints: $A_{eq}\chi = b_{eq}$. These equality constraints include generation-demand balance, i.e., the slack bus balancing equation and the relation between power injections and phase angles (1a). Matrix A_{eq} is not a full-rank matrix because of the slack bus balancing equation.

We start with eliminating θ . Without loss of generality, we assume that the balancing equation is the first equation in $A_{eq}\chi = b_{eq}$. First, we drop the balancing equation and θ^s variable. Also, assume that $s = 1$, i.e., the slack bus has index 1. In this case, the resulting $\tilde{A}_{eq}\tilde{\chi} = \tilde{b}_{eq}$ has a full-rank matrix. We will enforce the dropped constraint later. Let $\tilde{\chi}_\theta = (\theta^2, \dots, \theta^n)$, $\tilde{\chi}_{p_g} = (p_g^1, \dots, p_g^{n_g})$.

Thus

$$\tilde{A}_{eq}\tilde{\chi} = \tilde{b}_{eq} \iff [\tilde{A}_{eq,\theta}, \tilde{A}_{eq,p_g}] (\tilde{\chi}_\theta^\top, \tilde{\chi}_{p_g}^\top)^\top = \tilde{b}_{eq},$$

where $[\cdot, \cdot]$ is a horizontal stack, i.e., $\tilde{A}_{eq,\theta}$ contains only those columns that are related to θ solely, the similar applies for \tilde{A}_{eq,p_g} . Having said that, using the fact that $\tilde{A}_{eq,\theta}$ is a full-rank square matrix, we can eliminate phase angles:

$$\tilde{\chi}_\theta = (\tilde{A}_{eq,\theta})^{-1} (b_{eq} - \tilde{A}_{eq,p_g} p_g).$$

The power balance equation is as follows:

$$[A_{eq,\theta}^0, A_{eq,p_g}^0] (\tilde{\chi}_\theta^\top, \tilde{\chi}_{p_g}^\top)^\top = b_{eq}^0$$

Substituting the $\tilde{\chi}_\theta$, we get

$$\begin{aligned} & \left(-A_{eq,\theta}^0 (\tilde{A}_{eq,\theta})^{-1} \tilde{A}_{eq,p_g} + A_{eq,p_g}^0 \right) \tilde{\chi}_{p_g} = \\ & b_{eq}^0 - (A_{eq,\theta}^0)^\top \tilde{A}_{eq,\theta} b_{eq}. \end{aligned}$$

Denote $a_{ref}^\top = \left(-A_{eq,\theta}^0 (\tilde{A}_{eq,\theta})^{-1} \tilde{A}_{eq,p_g} + A_{eq,p_g}^0 \right) \in \mathbb{R}^{1 \times n_g}$ and $b_{ref} = b_{eq}^0 - (A_{eq,\theta}^0)^\top \tilde{A}_{eq,\theta} b_{eq}$, thus, one can define slack bus generation from the rest:

$$p_g^0 = \left(-(a_{ref}^{1:n_g})^\top p_g[1:] + b_{ref} \right) / a_{ref}^0,$$

where $x^{k_1:k_2}$ denotes the elements of vector x staring from k_1 ending on $k_2 - 1$, in the initial order. Next, we substitute the expressions obtained into inequalities to get $Wp_g \leq b$ formulation. Here we use superscript slices and indices for matrices, e.g., $(A'_{ineq})^0$ denote corresponding indexes for columns. Let $A_{ineq}\tilde{\chi} \leq b_{ineq}$ represent (1b). Then, substitution of the obtained expression for θ leads to an equivalent system of inequalities $A'_{ineq}p_g \leq b'_{ineq}$, where

$$A'_{ineq} = A_{ineq} - A_{ineq,\theta} \left(\tilde{A}_{eq,\theta} \right)^{-1} \tilde{A}_{eq,p_g}$$

and $b'_{ineq} = b'_{ineq} - A_{ineq,\theta} \left(\tilde{A}_{eq,\theta} \right)^{-1} \tilde{b}_{eq}$. Finally, we substitute the expression for the slack bus generation from the

balancing equation. This will lead to the final formulation $Wp_g \leq b$ with

$$W = (A'_{ineq})^0 a_{ref}^\top / a_{ref}^0 + (A'_{ineq})^{1:n_g},$$

$$\text{and } b = b'_{ineq} - (b_{ref} / a_{ref}^0) \cdot (A'_{ineq})^0.$$

The last step is the transformation of the linear cost function. Let $c(p_g) = c_1^\top p_g$. Then, the cost function after the transformation is $c^\top p_g^{1:n_g} + ct$ with $c = c_1^{1:n_g} - (c_1^0 / a_{ref}^0) a_{ref}^{1:n_g}$ and the cost correction term $ct = c_1^0 \cdot (b_{ref} / a_{ref}^0)$.